PHYSICAL REVIEW B VOLUME 31, NUMBER 12 15 JUNE 1985

$\mathbf{k}\cdot\mathbf{p}$ theory, effective-mass approach, and spin splitting for two-dimensional electrons in GaAs-GaAlAs heterostructures

R. Lassnig
Institute of Experimental Physics, University of Innsbruck, A-6020 Innsbruck, Austria
(Received 20 December 1984)

A five-level $\mathbf{k}\cdot\mathbf{p}$ theory is developed for conduction-band electrons in heterostructures. A local effective mass and a local g factor are obtained which depend on the variation of the p-type valence- and higher conduction-band edges. The effective mass and the spin splitting found in cyclotron and spin-resonance experiments are explained. A finite spin splitting is obtained at zero magnetic field and the possibility of determining the interface discontinuity from the spin splitting is discussed.

INTRODUCTION

To describe the band structure of semiconductors in the vicinity of extremal points, the so-called $\mathbf{k}\cdot\mathbf{p}$ perturbation theory has been developed by Luttinger and Kohn[1] and Kane.[2] The $\mathbf{k}\cdot\mathbf{p}$ theory is a semiempirical theory which uses several experimentally determined quantities (energy gap, effective mass, g factor) defined at a special point (mostly the Γ point) as an input. This technique allows one to determine the shape of the energy bands in the vicinity of the symmetry point to high accuracy without any need of complicated first-principles calculations. A reexamination of the $\mathbf{k}\cdot\mathbf{p}$ theory in III-V and II-VI compound semiconductors has been given by Hermann and Weisbuch.[3]

In $\mathbf{k}\cdot\mathbf{p}$ theory the effective band-edge mass is usually defined as the inverse second derivative of the quasiparticle (electron or hole) energy with respect to momentum at the valley extremum. Although this concept is quite evident for bulk electrons, it is not *a priori* clear if the effective-mass approach holds at surfaces or interfaces, where the energy-band structure is strongly modified and translational symmetry is not preserved.

However, experimental results from silicon metal-oxide-semiconducting (MOS) inversion layers show that the effective mass at the interface is equal to the bulk mass (many-body corrections at low densities neglected[4]). This is qualitatively explained by the properties of the electronic wave function: On the one hand the electron penetrates only very little into the oxide; on the other hand, the wave function spreads many unit cells into the bulk silicon. Hence the effective-mass approach can be well applied. A modified effective-mass equation has been derived by Sham and Nakayama.[5]

Band-structure calculations for narrow-gap semiconductor inversion layers with an infinite potential well have been performed by several authors.[6–8]

Within the last ten years a second class of structures containing quasi-two-dimensional electrons has been developed. By the successive deposition of adequately doped different semiconductor materials (such as GaAs-GaAlAs) heterostructures and superlattices have been prepared. The main quality restriction is the difference in the lattice parameters.

Especially for GaAs-GaAlAs, the conduction-band discontinuity is quite low, 250—300 meV,[9,10] so that the penetration of the electrons from the bulk GaAs into the barrier GaAlAs cannot be neglected. Self-consistent calculations of the energy bands including the penetration of the electrons into the GaAlAs have been recently performed by several authors,[11–14] who phenomenologically treated the bulk parameter variation in the two materials.

The purpose of the present paper is to describe the influence of band mixing (or nonparabolicity) in quantum wells on the electronic structure in detail. Electric and magnetic subband energies, the variation of the effective mass, and the spin splitting are calculated.

The formulation of $\mathbf{k}\cdot\mathbf{p}$ theory in two-dimensional (2D) systems with more or less abrupt material transitions requires careful handling of several physical problems.

First, the electron densities are high and a single-particle picture is not sufficient. Working within the Hartree approximation, this means that the total energy that has to be minimized is not the sum of the energies of the single particles, which obey the usual Schrödinger equation.

Second, a $\mathbf{k}\cdot\mathbf{p}$ Hamiltonian has to be derived which describes the transition between the two materials, by an adequate decomposition of the eigenstates into Bloch and envelope functions.

Third, the correct matching conditions of the wave functions across the interface have to be obeyed. A very useful study of model effective-mass Hamiltonians concerning this problem has been recently performed by Morrow and Brownstein.[15]

In contrast to elemental (or compound) semiconductors with an oxide interface the electrons in heterostructures are confined at the interface of quite similar materials. The variation of the crystal potential at the boundary is relatively small. Most important, the symmetry of the involved Bloch functions remains essentially unchanged. Therefore the loss of translational symmetry normal to the interface can be mathematically handled within the framework of $\mathbf{k}\cdot\mathbf{p}$ theory.

A three-level scheme is employed, which is extended to a five-level model by analogy. The calculation is restricted to compounds with an s-type conduction-band minimum at the Γ point. An 8×8 $\mathbf{k}\cdot\mathbf{p}$ matrix is derived and reduced to a coupled equation for the two spin components of the conduction band. The different contribu-

tions to the effective mass and to the g factor are discussed.

The variational wave functions used in the calculation are formally identical to those used by Ando[12] and Bastard.[13] The effective mass calculated for GaAs-$Ga_{0.7}Al_{0.3}As$ heterostructures is in good agreement with the experimental values of Seidenbusch *et al.*[16] The possibility of determining the conduction-band discontinuity from the spin splitting is discussed. The experimental results of Stein and Klitzing[17] are qualitatively well described. It is demonstrated that from the variation of the effective g factor due to light illumination the origin of additionally created inversion layer electrons can be determined.

HARTREE APPROXIMATION

The Hartree Hamiltonian for the interacting electron gas is given by

$$H_H=\sum_i \left[T^i+V^i_{\rm ext}+\tfrac{1}{2}\sum_{j\neq i} W_{ij} \right] , \tag{1}$$

where the first two terms denote the kinetic energy and the external potential acting on the ith particle. The double sum over W_{ij} is the self-interaction of the electron gas.

Eigenstates $|\phi\rangle$ of the system are represented as a product of single-particle wave functions:

$$|\phi\rangle=\prod_i |\varphi_i\rangle . \tag{2}$$

Varying $(\langle H_H\rangle-\lambda\langle\phi|\phi\rangle)$ with respect to the wave function $|\varphi_i\rangle$, one obtains the single-particle Hamiltonian:

$$\left[T^i+V^i_{\rm ext}+\sum_{j\neq i}\langle\varphi_j|W_{ij}|\varphi_j\rangle \right] |\varphi_i\rangle=\lambda_i|\varphi_i\rangle . \tag{3}$$

The constants λ_i are easily identified with the single-particle energies of the system. Whereas Eq. (3) is the Schrödinger equation that can be integrated, the total energy E that has to be minimized is

$$E=\sum_i \lambda_i-\tfrac{1}{2}\sum_{i\neq j}\langle\varphi_i,\varphi_j|W_{ij}|\varphi_i,\varphi_j\rangle . \tag{4}$$

For **k·p** theory, this distinction is essential, since it is the single-particle Hamiltonian that has to be diagonalized. Finally, it should be noted that the exclusion $(i\neq j)$ is irrelevant for the considered system, where the electron densities are high.

k·p THEORY FOR HETEROSTRUCTURES

In a heterostructure with the interface in the $z=0$ plane the band structure is determined by the following single-particle Hamiltonian:

$$\mathscr{H}=\hat{P}^2/2m_0+V_0(\mathbf{x})+V(z),\quad V(z)=V_H(z)+V_D(z) . \tag{5}$$

$\hat{P}$ denotes the momentum operator and m_0 is the free-electron mass. $V_0(\mathbf{x})$ is the crystal potential which includes also the material change at the boundary. The long-range potential $V(z)$ includes the depletion

$$V_D(z)=\frac{4\pi e^2}{\kappa_s}N_d z , \tag{6}$$

and the Hartree contributions

$$V_H(z)=\frac{4\pi e^2}{\kappa_s}N_{\rm el}\left[z-\int_{-\infty}^{z}\rho(z')(z-z')dz' \right] \tag{7}$$

of the electrons. κ_s is the static dielectric constant, which is assumed to be material independent. N_d and $N_{\rm el}$ denote the depletion and inversion charge, and $\rho(z)$ is the normalized electronic charge density. Image charge effects are neglected, since their influence on the subband energies is very small.[14]

Figure (1a) shows schematically the energy band structure near the Γ point ($k=0$) in a cubic direct-gap semiconductor. The main contributions to nonparabolicity in the s-type conduction band arise from mixing with the valence and the higher conduction band, which are both p type. Figure (1b) shows the potential distribution in a heterostructure. The steps in the conduction band, the valence band, and the spin-split band are denoted by δ_c, δ_v, and δ_Δ. For simplicity the higher conduction band is not indicated.

In the following the **k·p** matrix is derived for a three-level model to keep the analytical expressions short. In the final formulas, however, the full five-band expressions will be used.

Before investigating the heterostructure case, the principles of **k·p** theory are shortly reviewed: The first step of **k·p** theory is to develop the electronic wave function $\varphi(k)$ in the vicinity of the symmetry point in terms of the symmetric Bloch functions $u_{l,0}$:

$$\varphi(k)=\sum_l u_l(0)f_l(k) . \tag{8}$$

The functions $u_{l,0}$ have the symmetry of the direct lattice, oscillate rapidly, and satisfy the band-edge equation:

$$[\hat{P}^2/2m_0+V_0(\mathbf{x})-\epsilon_{l,0}]u_l(0)=0 . \tag{9}$$

The envelope functions $f_l(k)$ are slowly varying and describe the band mixing away from the symmetry point. The index l goes, at least in principle, over all energy bands of the crystal. For practical calculations, however, only the nearest energy bands contribute. The present calculation is for an s-type conduction band, which mainly interacts with its neighboring p-type valence and higher conduction band.

The second step of **k·p** theory is to multiply the Schrödinger equation:

$$\sum_l \left[\frac{1}{2m_0}(\hat{P}^2u_l)+\frac{1}{m_0}(\hat{P}u_l)\hat{P}+\frac{u_l}{2m_0}\hat{P}^2+V_0(\mathbf{x})u_l \right] f_l =\epsilon\sum_l f_l u_l \tag{10}$$

from the left with $u_{m,0}$ and to integrate over the unit cells. The envelope functions $f_l(k)$ are assumed to be constant over the unit cell. They are taken out of the integral and one obtains a matrix equation for the $f_m(k)$:

$$
\begin{array}{c|cccccccc|c}
 & \kappa\hat{P}_+ & (\frac{1}{3})^{1/2}\kappa\hat{P}_- & 0 & (\frac{2}{3})^{1/2}\hat{P}_z\kappa & & & & & f_1 \\
\kappa\hat{P}_- & \left[-\epsilon+U_v+\frac{\hat{P}^2}{2m_0}\right] & 0 & 0 & 0 & & & & & f_3 \\
(\frac{1}{3})^{1/2}\kappa\hat{P}_+ & 0 & \left[-\epsilon+U_v+\frac{\hat{P}^2}{2m_0}\right] & (\frac{2}{3})^{1/2}\kappa\hat{P}_z & 0 & & & & & f_5 \\
-(\frac{2}{3})^{1/2}\kappa\hat{P}_+ & 0 & \left[-\epsilon+U_\Delta+\frac{\hat{P}^2}{2m_0}\right] & (\frac{1}{3})^{1/2}\kappa\hat{P}_z & 0 & & & & & f_7 \\
0 & 0 & (\frac{2}{3})^{1/2}\kappa\hat{P}_z & \left[-\epsilon+U_c+\frac{\hat{P}^2}{2m_0}\right] & \kappa\hat{P}_- & & & & & f_2 \\
0 & 0 & 0 & \kappa\hat{P}_+ & \left[-\epsilon+U_v+\frac{\hat{P}^2}{2m_0}\right] & -(\frac{1}{3})^{1/2}\kappa\hat{P}_+ & & & & f_4 \\
(\frac{2}{3})^{1/2}\kappa\hat{P}_z & 0 & 0 & -(\frac{1}{3})^{1/2}\kappa\hat{P}_- & 0 & \left[-\epsilon+U_v+\frac{\hat{P}^2}{2m_0}\right] & & & & f_6 \\
(\frac{1}{3})^{1/2}\kappa\hat{P}_z & 0 & 0 & (\frac{2}{3})^{1/2}\kappa\hat{P}_- & 0 & 0 & \left[-\epsilon+U_\Delta+\frac{\hat{P}^2}{2m_0}\right] & & & f_8 \\
\end{array}
=0 \qquad (13)
$$

$$\sum_l [(\hat{P}^2/2m_0+\epsilon_{l,0}-\epsilon)\delta_{lm}+\hat{\kappa}_{lm}\hat{P}]f_l=0\ . \qquad (11)$$

Here the momentum matrix elements between the interacting bands have been abbreviated with $\hat{\kappa}_{lm}$ and Eq. (9) has been used. Equation (11) can be solved by matrix diagonalization.[18]

In a heterostructure, $\mathbf{k}\cdot\mathbf{p}$ theory can be applied based on the following arguments: For most semiconductor heterostructures, such as GaAs-GaAlAs, the difference of the lattice constants is small. For a particle the boundary represents mainly a change of the rapidly oscillating crystal potential. Neglecting lattice mismatch, the symmetry of the two materials is identical and the Bloch functions are very similar.

Therefore the complete wave function is expanded in the regime of GaAs unit cells by GaAs Bloch functions and in the barrier regime by GaAlAs Bloch functions. The continuity conditions for the wave function can be fulfilled without drastic changes at the boundaries for the two sets of unit cells.

Without any detailed knowledge of the real wave functions, $\mathbf{k}\cdot\mathbf{p}$ theory generally uses the integral over the unit cell like a continuous variable (with respect to the envelope function). The same principle can also be applied to the 2D system: The Bloch function integrals over the unit cells on both sides of the boundary represent mean values over a few angströms. The transition between the two media can therefore, in the $\mathbf{k}\cdot\mathbf{p}$ picture, be taken into account by a continuous function $h(z)$ leading from the GaAs values to the GaAlAs values:

$$\varphi=\sum_l f_l(z)\{u_l^{\mathrm{GaAs}}[1-h(z)]+u_l^{\mathrm{GaAlAs}}h(z)\}\ . \qquad (12)$$

The transition is, of course, not an abrupt one, since mean values have to be formed. The description by an abrupt step function is therefore only justified if the penetration of the electronic wave function into the barrier material significantly exceeds the unit cell diameter.

At this point it is useful to mention that, although for the ternary alloy GaAlAs a simple unit cell does not exist in principle, the averaging procedure over several GaAs- and AlAs-atom pairs leads to a well-defined band structure. Deviations from the average composition can be described as alloy disorder scattering. This illustrates that also the transitions from the GaAs band structure to the GaAlAs band structure can be analogously described by a relatively smooth function $h(z)$.

The exact band-edge functions $u_{l,0}$ as well as the detailed change of the s- and p-type functions from the GaAs band structure to the GaAlAs band structure are unknown. Therefore it is assumed that the s-type wave functions are similar in both materials, and that the main changes occur in the p-type functions.

In the following derivation a magnetic field H normal to the interface is also included, working in the Landau gauge. Using the nomenclature of Zawadzki[18] (see Appendix A) and using the band-edge equations for the Bloch functions of both materials, the $\mathbf{k}\cdot\mathbf{p}$ matrix is obtained as Eq. (13), shown at left.

$\hat{P}_z=-i\hbar\partial_z$ and $\hat{P}_\pm=(\hat{P}_x\pm i\hat{P}_y)/\sqrt{2}$ are generalized momentum operators. $\kappa=i\langle s\,|\,\partial_z\,|\,p_z\rangle$ denotes the

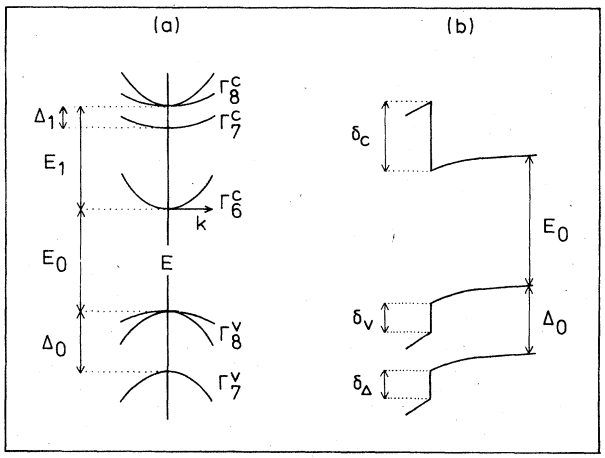

FIG. 1. (a) Energy band structure at the Γ point in five-level approximation. (b) Band edges in a heterostructure with abrupt interface (the higher conduction band is not indicated).

momentum matrix element of the Bloch functions. U_c, U_v, and U_Δ represent the potentials of the conduction band, the valence band, and the spin-split band, including the potential step:

$$U_c(z)=V(z)+\delta_c h(z) , \tag{14}$$

$$U_v(z)=V(z)-E_0-\delta_v h(z) , \tag{15}$$

$$U_\Delta(z)=V(z)-E_0-\Delta-\delta_\Delta h(z) . \tag{16}$$

The matrix equation (13) is resolved by substitution, ending up with two coupled equations for the spin-up and the spin-down conduction band:

$$\begin{bmatrix} \mathscr{H}_0+\mathscr{H}_s-\epsilon & \mathscr{H}_{12} \\ \mathscr{H}_{21} & \mathscr{H}_0-\mathscr{H}_s-\epsilon \end{bmatrix} \begin{bmatrix} f_1 \\ f_2 \end{bmatrix} =0 , \tag{17}$$

where

$$\mathscr{H}_0=U_c+\hat{P}\frac{1}{2m(z)}\hat{P} , \tag{18}$$

$$\frac{1}{2m(z)}=\frac{\kappa^2}{3}\left[\frac{2}{N}+\frac{1}{M}\right]+\frac{1}{2m_0} , \tag{19}$$

$$\mathscr{H}_s=\mu_B g^*(z)H=\mu_B H-\frac{\kappa^2}{3}\frac{\hbar^2}{l^2}\left[\frac{1}{N}-\frac{1}{M}\right] , \tag{20}$$

$$\mathscr{H}_{12}=-i\frac{\hbar}{\sqrt{2}}\frac{dg^*(z)}{dz}\hat{P}_- , \tag{21}$$

$$\mathscr{H}_{21}=\mathscr{H}_{12}^+ , \tag{22}$$

$$N=\epsilon-U_v , \tag{23}$$

$$M=\epsilon-U_\Delta . \tag{24}$$

In the energy denominators N,M, the kinetic term $\hat{P}^2/2m_0$ has been neglected. The diagonal term H_0 determines the basic band structure. It can be seen that the Hamiltonian is Hermitian. The form $\hat{P}[1/2m(z)]\hat{P}$ is identical to that obtained by Ben Daniel and Duke,[19] who derived it from current conservation.

The local effective mass $m(z)$ still depends self-consistently on the separation of the energy eigenvalue ϵ from the z-dependent valence band edges U_v and U_Δ. The same is true for the local effective g factor $g^*(z)$. The nondiagonal terms H_{12} and H_{21} contain the ladder operators $\hat{P}_\pm$, which means that only adjacent Landau levels are coupled. For zero magnetic field, these contributions lead to a finite spin-splitting for nonzero parallel wave vector.

EFFECTIVE MASS

Neglecting spin splitting, the Schrödinger equation for the electron motion in the conduction band is

$$\left[U_c+\hat{P}\frac{1}{2m(z)}\hat{P}-\epsilon\right]|\varphi\rangle=0 . \tag{25}$$

In a three-level model, $m(z)$ is simply given by Eq. (19). However, since we are interested in a more exact approximation to obtain reasonable quantitative results, we include also the contributions of the higher lying energy levels. Following Weisbuch and Hermann[3] the next higher p-type conduction band is explicitly included in a five-level approximation, whereas the influence of the remaining energy bands is included in a constant factor C_m:

$$\frac{m_0}{m(z)}=1+C_m+\frac{P_v^2}{3}\left[\frac{2}{N}+\frac{1}{M}\right]-\frac{P_c^2}{3}\left[\frac{2}{N'}+\frac{1}{M'}\right] . \tag{26}$$

Here the band edges of the higher conduction band have been denoted by U_c' and U_Δ':

$$N'=U_c'-\epsilon, \quad U_c'=E_1+\delta_c' h(z)+V(z) \tag{27}$$

$$M'=U_\Delta'-\epsilon_1, \quad U_\Delta'=E_1+\Delta_1+\delta_\Delta' h(z)+V(z) . \tag{28}$$

The momentum matrix elements have been transformed into $P_v^2=2\kappa_v^2 m_0$, $P_c^2=2\kappa_c^2 m_0$ for the valence and the higher conduction band, respectively. In the present paper interface grading is not discussed, and the transition function $h(z)$ will be replaced by the step function $\Theta(-z)$.

For better analytic handling, the z dependence of the effective mass is rewritten in the form

$$\frac{1}{m(z)}=\frac{1}{m_0^*}\left[\frac{1}{1+\delta m\Theta(-z)}-[\epsilon-V(z)]\alpha(z)+O[(\epsilon-V)\alpha]^2\right] , \tag{29}$$

where for a semiconductor with $\epsilon-V(z)\ll E_0$ the last expression can be neglected and the other parameters are given by

$$\frac{m_0}{m_0^*}=1+C_m+\frac{P_v^2}{3}\left[\frac{2}{E_0}+\frac{1}{E_0+\Delta_0}\right]-\frac{P_c^2}{3}\left[\frac{2}{E_1}+\frac{1}{E_1+\Delta_1}\right], \tag{30}$$

$$\delta m=\left[1+C_m+\frac{P_v^2}{3}\left[\frac{2}{E_0+\delta_v}+\frac{1}{E_0+\Delta_0+\delta_\Delta}\right]+\frac{P_c^2}{3}\left[\frac{2}{E_1+\delta_c'}+\frac{1}{E_1+\Delta_1+\delta_\Delta'}\right]\right]^{-1}-1, \tag{31}$$

$$\alpha(z)=\alpha_-\Theta(-z)+\alpha_+\Theta(z), \tag{32}$$

$$\alpha_+=\frac{m_0^*}{3m_0}\left[P_v^2\left[\frac{2}{E_0^2}+\frac{1}{(E_0+\Delta_0)^2}\right]+P_c^2\left[\frac{2}{E_1^2}+\frac{1}{(E_1+\Delta_1)^2}\right]\right], \tag{33}$$

$$\alpha_-=\frac{m_0^*(1+2\delta m+\delta m^2)}{3m_0}\left[P_v^2\left[\frac{2}{(E_0+\delta_v)^2}+\frac{1}{(E_0+\Delta_0+\delta_\Delta)^2}\right]+P_c^2\left[\frac{2}{(E_1+\delta_c')^2}+\frac{1}{(E_1+\Delta_1+\delta_\Delta')^2}\right]\right]. \tag{34}$$

m_0^* is the three-dimensional band-edge mass of the bulk semiconductor, δm is the variation at the interface, and $\alpha(z)$ describes the additional influence of the nonparabolic band mixing. The factor $\delta m\Theta(-z)$ does not represent the discontinuity to the effective mass of the barrier material, but is only dependent on the steps of the neighboring band-edge energies.

For the (x,y)-dependent part of the wave function, harmonic oscillator solutions $|\,n\,\rangle$ are used:

$$|\,\varphi\,\rangle=|\,n\,\rangle\varphi(z). \tag{35}$$

Multiplying Eq. (25) from the left with φ^* and integrating over x space, one obtains the following expression for an electron in the nth Landau level (where $\omega_c=eH/m_0^*c$ denotes the bulk cyclotron frequency):

$$\epsilon_n=\langle U_c\rangle+\hbar\omega_c(n+\tfrac{1}{2})\left\langle\frac{m_0^*}{m(z)}\right\rangle+\left\langle\hat{P}_z\frac{1}{2m(z)}\hat{P}_z\right\rangle. \tag{36}$$

The brackets $\langle\ \rangle$ denote the expectation value with respect to the envelope function $\varphi(z)$. The electron energy ϵ_n is given by

$$\epsilon_n=\frac{\hbar\omega_c(n+\frac{1}{2})\left[\left\langle\frac{1}{1+\delta m\Theta(-z)}\right\rangle+\langle V\alpha\rangle\right]+\langle U_c\rangle+\frac{1}{2m_0^*}\left\langle\hat{P}_z\left[\frac{1}{1+\delta m\Theta(-z)}+V\alpha\right]\hat{P}_z\right\rangle}{1+\hbar\omega_c(n+\frac{1}{2})\langle\alpha\rangle+\frac{1}{2m_0^*}\langle\hat{P}_z\alpha\hat{P}_z\rangle}. \tag{37}$$

The kinetic energy terms are corrected with respect to their "bulk" values. This correction can be either positive or negative, depending on the signs of the neighboring band discontinuities. This result is in contrast to the phenomenological assumption of a local effective mass, which varies proportional to the barrier material values.

Besides intersubband experiments, the best information on the energy levels is obtained from cyclotron-resonance experiments. The relative change of the energy separation between adjacent Landau levels is interpreted as a variation of the effective mass:

$$m^*(n\to n+1)=m_0^*\frac{\hbar\omega_c}{\epsilon_{n+1}-\epsilon_n}. \tag{38}$$

Inserting Eq. (36) into Eq. (38) and keeping only the leading terms of the nonparabolicity, the effective mass in a heterostructure can be written as

$$\frac{m^*(n\to n+1)}{m_0^*}=\left[1+(2n+2)\hbar\omega_c\langle\alpha\rangle+\langle P_z\alpha P_z\rangle\frac{1}{2m_0^*}\right]\left[1-\rho_-+\frac{\rho_-}{1+\delta m}\right]$$
$$+\frac{\langle\alpha\rangle}{2m_0^*}\left\langle P_z\frac{1}{1+\delta m\Theta(-z)}P_z\right\rangle+\langle\alpha\rangle\delta_c\rho_-+\langle V\rangle\langle\alpha\rangle-\langle V\alpha\rangle. \tag{39}$$

The contributions to the effective mass are easily identified: The expression $\rho_-=\langle\Theta(-z)\rangle$ is the amount of charge density penetrating into the barrier. The kinetic terms show the typical nonparabolicity behavior, where the factor $\langle\alpha\rangle$ corresponds to an effective gap. The direct influence of the potential $\langle V\rangle$ is very small, since the last expression cancels. The present result demonstrates that the kinetic terms, represented by differential operators, couple the s- and p-type bands together and are responsible for the nonparabolicity. In other words, the smooth potential $V(z)$ mainly quantizes the motion and thereby increases the kinetic contributions.

VARIATIONAL SOLUTION AND MATCHING CONDITIONS

Until now, the exact wave functions have not been determined. It should be kept in mind that, although the single-particle Schrödinger equation (25) holds, the total energy of the system that has to be minimized is given by

$$E_{\rm tot}=\sum_i \epsilon_i-\frac{N_{\rm el}}{2}\langle V_H\rangle \ . \tag{40}$$

In principle, Eq. (25) has to be integrated numerically. In the present paper, appropriate variational wave functions are used, which have been demonstrated by Ando[12] to yield very accurate energies for the zeroth electric subband. Thus, our task is to evaluate the expectation values $\langle\ \rangle$ and to minimize the total energy with respect to the variational parameters.

Before doing that, however, we investigate the matching conditions at the interface. Morrow and Brownstein[15] have pointed out that since the right-hand side of

$$\left[\frac{d}{dz}\frac{1}{m(z)}\frac{d}{dz}\right]\varphi(z)=\frac{2}{\hbar^2}(U_c-\epsilon)\varphi(z) \tag{41}$$

is finite for all z, the left-hand side must be similarly well behaved. This implies that, integrating from $-\delta$ to $+\delta$ and taking the limit $\delta\to 0$, the expression

$$\frac{1}{m(z)}\frac{d\varphi}{dz} \tag{42}$$

is continuous at $z=0$. In other words, although the absolute value of the envelope function $\varphi(z)$ is continuous, the derivative $d\varphi(z)/dz$ is discontinuous, where the step is determined by the abrupt variation of the effective mass:

$$\frac{d\varphi}{dz}(z=0^-)=(1+\delta m)\frac{d\varphi}{dz}(z=0^+) \ . \tag{43}$$

The nondifferentiability of the envelope function at the interface is due to the step-function approximation, whereas a more realistic graded interface would yield an adequately smooth behavior.

Finally, the trial wave functions are given by[12]

$$\varphi(z)=\begin{cases}\sqrt{Bb}\,(zb+k)e^{-bz/2}, & z>0\\ \sqrt{Cc}\,e^{cz/2}, & z<0\ .\end{cases} \tag{44}$$

Using the matching conditions at $z=0$ and requiring normalization, three of the five parameters can be directly expressed in terms of the two remaining trial parameters b and k:

$$c=b(2-k)(1+\delta m)/k \ , \tag{45}$$

$$B=c/[bk^2+c(2+2k+k^2)] \ , \tag{46}$$

$$C=Bbk^2/c \ . \tag{47}$$

The expectation values $\langle\ \rangle$ are listed in Appendix B.

SPIN SPLITTING

The spin splitting is determined by the Pauli-spin term H_s and by the nondiagonal parts of the Hamiltonian, which are proportional to the ladder operators $\hat{P}_\pm$:

$$\begin{bmatrix}\mathscr{H}_0+\mathscr{H}_s-\epsilon & -i\frac{\hbar}{\sqrt{2}}\frac{dg^*(z)}{dz}\hat{P}_-\\ i\frac{\hbar}{\sqrt{2}}\frac{dg^*(z)}{dz}\hat{P}_+ & \mathscr{H}_0-\mathscr{H}_s-\epsilon\end{bmatrix}\begin{bmatrix}f_1\\ f_2\end{bmatrix}=0 \ , \tag{48}$$

$$\mathscr{H}_s=\tfrac{1}{2}\mu_B g^*(z)H \ , \tag{49}$$

$$\frac{g^*(z)}{2}-1=\left[-\frac{P_v^2}{3}\right]\left[\frac{1}{N}-\frac{1}{M}\right]+\frac{P_c^2}{3}\left[\frac{1}{N'}-\frac{1}{M'}\right]+C_g \ . \tag{50}$$

In analogy to the local effective mass Eq. (26), also the contributions of the higher conduction bands (including a constant factor C_g) to the local g factor $g^*(z)$ are taken into account. The g factor is now rewritten in the form

$$g^*(z)=g_0^*+\delta g^*\Theta(-z)-\beta(z)V(z) \ , \tag{51}$$

where

$$g_0^*=2\left[1+C_g-\frac{P_v^2}{3}\left[\frac{1}{E_0+\epsilon}-\frac{1}{E_0+\Delta_0+\epsilon}\right]+\frac{P_c^2}{3}\left[\frac{1}{E_1-\epsilon}-\frac{1}{E_1+\Delta_1-\epsilon}\right]\right] , \tag{52}$$

$$\delta g^*=2\left[1+C_g-\frac{P_v^2}{3}\left[\frac{1}{E_0+\delta_v+\epsilon}-\frac{1}{E_0+\Delta_0+\delta_\Delta+\epsilon}\right]+\frac{P_c^2}{3}\left[\frac{1}{E_1+\delta_c'-\epsilon}-\frac{1}{E_1+\Delta_1+\delta_\Delta'-\epsilon}\right]\right]-g_0^* \ , \tag{53}$$

and

$$\beta(z)=\beta_-\Theta(-z)+\beta_+\Theta(z) \ , \tag{54}$$

$$\beta_+=\frac{2}{3}\left[P_v^2\left[\frac{1}{(E_0+\epsilon)^2}-\frac{1}{(E_0+\Delta_0-\epsilon)^2}\right]+P_c^2\left[\frac{1}{(E_1-\epsilon)^2}-\frac{1}{(E_1+\Delta_1-\epsilon)^2}\right]\right] , \tag{55}$$

$$\beta_-=\frac{2}{3}\left[P_v^2\left[\frac{1}{(E_0+\delta_v+\epsilon)^2}-\frac{1}{(E_0+\Delta_0+\delta_\Delta+\epsilon)^2}\right]+P_c^2\left[\frac{1}{(E_1+\delta_c'-\epsilon)^2}-\frac{1}{(E_1+\Delta_1+\delta_\Delta'-\epsilon)^2}\right]\right] . \tag{56}$$

If the spin splitting is not too large, the energy ϵ can be kept constant in the denominators.

For the envelope functions (f_1,f_2), the following ansatz is chosen:

$$\begin{bmatrix} f_1 \\ f_2 \end{bmatrix} = \begin{bmatrix} c_1 \mid n \rangle \\ c_2 \mid n+1 \rangle \end{bmatrix} \varphi(z) , \tag{57}$$

where the separability of the (x,y)-dependent part greatly simplifies the calculation. The z-dependent part is again represented by the variational wave function $\varphi(z)$.

Taking expectation values $\langle\ \rangle$ with $\varphi(z)$, two linear equations are obtained for the coefficients c_1 and c_2. The resulting energy levels are given by

$$\epsilon_n^{\pm} = \langle U_c \rangle + \left\langle \hat{P}_z \frac{1}{2m(z)} \hat{P}_z \right\rangle + \hbar\omega_c (n+1) \pm \left[\left[\frac{\hbar\omega_c}{2} - \langle \mathscr{H}_s \rangle \right]^2 + \left[n(n+1) \left| \left\langle \frac{dg^*}{dz} \right\rangle \right|^2 \frac{\hbar^4}{8m_0^2 l^2} \right]^{1/2} \right]^{1/2} \tag{58}$$

and the spin splitting is determined by subtracting:

$$\epsilon_{n+1}^- - \epsilon_n^+ \cong 2\langle \mathscr{H}_s \rangle + \frac{\hbar^2}{8m_0^2} \left| \left\langle \frac{dg^*}{dz} \right\rangle \right|^2 \frac{\hbar^2}{l^2} \sqrt{n+1} (\sqrt{n} + \sqrt{n+2}) / (\hbar\omega_c - 2\langle \mathscr{H}_s \rangle) . \tag{59}$$

At zero magnetic field the Pauli-spin term vanishes, the oscillator functions $\mid n \rangle$ must be replaced by $\exp(ik_x x + ik_y y)$, and the residual spin splitting is given by

$$\epsilon_{k_\perp}^+ - \epsilon_{k_\perp}^- = \frac{\hbar^2 k_\perp}{2m_0} \left\langle \frac{dg^*}{dz} \right\rangle . \tag{60}$$

The loss of inversion symmetry leads to a finite spin splitting also at zero magnetic field, at least for nonzero parallel wave vector $k_\perp$. This result is in good agreement with recent spin-resonance experiments of Stein and Klitzing.[17]

The variational matrix elements for the diagonal term $\langle \mathscr{H}_s \rangle$ are listed in Appendix B. The evaluation of the expectation value $\langle dg^*(z)/dz \rangle$ can be performed without detailed knowledge of the wave function. For a bound state the mean value of the electric field vanishes and the relation

$$\left\langle \frac{dU_c}{dz} \right\rangle = \left\langle \frac{dV(z)}{dz} \right\rangle + \delta_c \left\langle \frac{d\Theta(-z)}{dz} \right\rangle \cong 0 \tag{61}$$

holds. The expectation value for the slowly varying electric field $dV(z)/dz$ is given by

$$\left\langle \frac{dV(z)}{dz} \right\rangle = \frac{4\pi e^2}{\kappa_s} (N_d + \tfrac{1}{2} N_{\rm el}) . \tag{62}$$

Therefore also the derivative of the transition function $\langle d\Theta(-z)/dz \rangle$ can be obtained by combining Eqs. (61) and (62):

$$\left\langle \frac{d\Theta(-z)}{dz} \right\rangle = \frac{4\pi e^2}{\kappa_s \delta_c} (N_d + \tfrac{1}{2} N_{\rm inv}) . \tag{63}$$

The matrix element $\langle dg^*(z)/dz \rangle$ contains the same expressions as the above equations, only the conduction-band potential is replaced by the valence-band potential. The nondiagonal spin-splitting factor can therefore be evaluated to be

$$\left| \left\langle \frac{dg^*}{dz} \right\rangle \right| \cong \frac{4\pi e^2}{\kappa_s} (N_d + \tfrac{1}{2} N_{\rm el}) \times \left[\frac{\delta g^*}{\delta_c} + \beta_+ + \rho_- (\beta_- - \beta_+) \frac{N_d + N_{\rm el}}{N_d + \tfrac{1}{2} N_{\rm el}} \right] . \tag{64}$$

DISCUSSION

A $\mathbf{k}\cdot\mathbf{p}$ Hamiltonian has been derived to describe the electronic structure of two-dimensional systems in semiconductor quantum wells. Many-body effects are included in the Hartree approximation, where the single-particle Hamiltonian is diagonalized within the framework of $\mathbf{k}\cdot\mathbf{p}$ theory. The kinetic energy is of the form $\hat{P}\{1/[2m(z)]\}\hat{P}$. $m(z)$ is a local effective mass, which depends on the energy separation of the electron from the neighboring p-type bands. Analogously, a z-dependent g-factor $g^*(z)$ is defined. The spin splitting is increased by a nondiagonal contribution, which couples adjacent Landau levels and remains finite even for zero magnetic field.

The calculations are performed with the help of variational wave functions. If the interface is approximated by an abrupt step function, the slope of the envelope function is discontinuous at $z=0$, and the variation is proportional to the local effective mass variation.

Cyclotron- and spin-resonance experiments measure to a high accuracy the nonlinearities of the energy separation between neighboring Landau levels and spin levels. The nonparabolic energy fine structure is usually described in terms of an effective-mass and g factor variation.

The theoretical results are discussed for GaAs-$Ga_{0.7}Al_{0.3}As$ heterostructures, where the theory can be tested by high precision experimental data. In the GaAs-GaAlAs system the energy gap is so large that the quantities ϵ and $V(z)$ can be well expanded when appearing in the denominator. Therefore all the relevant matrix elements can be evaluated analytically and the numerical work is reduced to the total-energy minimization with respect to the variational parameters. However, it is necessary to mention that for very-low-gap materials, such as InSb, these approximations are misleading and Eq. (25) must be integrated numerically. Another advantage of the GaAs system is that at low temperatures and not-too-high electron densities only the lowest electric subband is occupied, which greatly simplifies the calculations.

The band-structure parameters for the GaAs and the $Ga_{0.7}Al_{0.3}As$ are given in Table I.[20] The constants C_m and C_g are taken to be $C_m = -1.8$ and $C_g = -0.01$. The momentum matrix elements $P_v^2 = 28.9$ eV and $P_c^2 = 6$ eV and the static dielectric constant $\kappa_s = 12.8$ are assumed to

TABLE I. Band-edge parameters E_0, E_1, Δ_0, Δ_1 (all in meV), effective mass m_0^* (in units of m_0), and effective g factor g_0^* for GaAs and $Ga_{0.7}Al_{0.3}As$ (Ref. 20).

	E_0	E_1	Δ_0	Δ_1	m_0^*	g_0^*
GaAs	1519	3140	341	−171	0.066	−0.44
$Ga_{0.7}Al_{0.3}As$	1900	2842	310	−171	0.086	0.45

be equal for the two materials.

The exact barrier height for the conduction band is not very well known. Furthermore, it can be sample dependent, since the epitaxial formation of a barrier depends on the growth conditions. For high-quality samples, the usually accepted value is 85%,[9] whereas some new experiments with p-type channels indicate a lower value.[10] In the following also the possible determination of the barrier height from the energy fine structure and the nonparabolicity sum rules will be discussed.

A. Effective mass

The dependence of the effective mass on the material parameters and on the charge densities is derived in Eq. (39). With respect to the bulk value, it is mainly changed by two contributions: First, the electron penetrates into the barrier material and "feels" the local variation of the band-edge parameters. The conduction-band step always leads to an increase of the effective mass. The influence of the valence band and of the higher conduction-band discontinuities can be either positive or negative, depending on the material parameters. Altogether, these contributions are similar, but not equal to the variation of the bulk effective mass. Second, the kinetic terms contribute similarly as in three dimensions. The direct influence of the slowly-varying potential $V(z)$ is negligible. This is qualitatively explained by the fact that the potential only quantizes the electron motion, whereas the increase of the kinetic energy couples the s- and p-type bands together.

Figure 2 shows the amount of charge density penetrating into the GaAlAs barrier as a function of the barrier height, which is normalized with respect to the fundamental gap difference $\delta E_g = E_0(Ga_{0.7}Al_{0.3}As) - E_0(GaAs)$ of the two materials, for $N_{el} = 3\times10^{11}/cm^2$ and for two depletion charge values. The increase of ρ_- with decreasing δ_c is significant, but the absolute value is just a few percent. A stronger background (depletion) field also increases the penetration into the GaAlAs.

Figure 3 shows the effective mass for the (0−1) cyclotron-resonance transition at $H = 6$ T as a function of the electron density for two depletion charge densities and $\delta_c/\delta E_g = 85\%$ (solid line) and $\delta_c/\delta E_g = 60\%$ (dashed line). It can be seen that the effective mass is more sensitive to the depletion charge than to the inversion charge, whereas the δ_c dependence is very weak. The absolute value of the effective mass agrees well with the experimental value of Seidenbusch *et al.*[16] Unfortunately, the experimental uncertainty of the depletion charge density makes the determination of δ_c via the effective mass practically impossible. However, the dependence of the effective mass on the potential is important if other fine-structure effects such as polaron interaction are studied.

B. Effective g factor

A local g factor $g^*(z)$ has been defined which depends on the potential variation of the valence and the higher conduction band in the z direction. At high magnetic fields the Pauli term $\mu_B\langle g^*(z)\rangle H$ dominates the spin splitting. The nondiagonal term is proportional to $\langle dg^*(z)/dz\rangle \hat{P}_\pm$ and couples adjacent Landau levels.

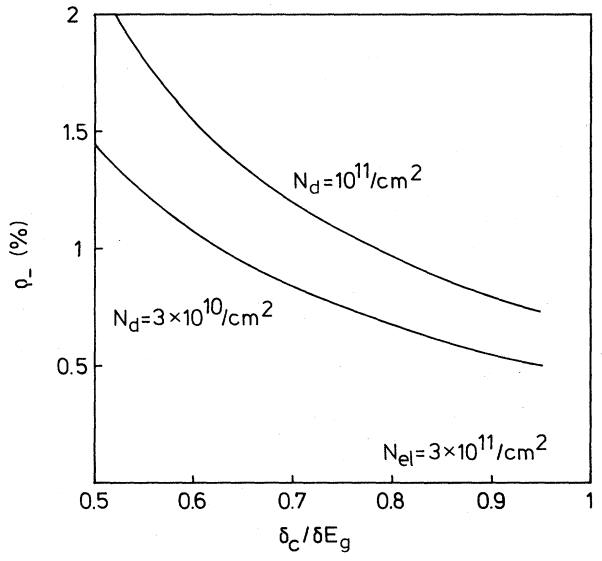

FIG. 2. Charge density ρ_- penetrating into the GaAlAs as a function of the barrier height, for $N_{el} = 3\times10^{11}/cm^2$ and for two depletion charge densities.

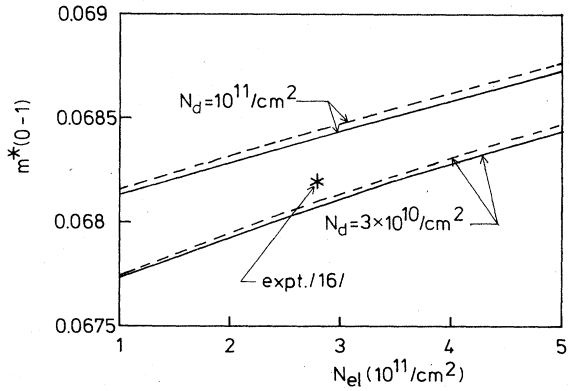

FIG. 3. Effective mass for the (0−1) cyclotron resonance transition as a function of electron density, for two N_d values and $\delta_c/\delta E_g = 85\%$ (solid line) and $\delta_c/\delta E_g = 60\%$ (dashed line). The experimental value (*) is taken from Ref. 16.

Therefore the nondiagonal contribution to the spin splitting is stronger at low magnetic fields, where ω_c becomes small. For $k_\perp \neq 0$, the splitting remains finite even at zero magnetic field. The present theory is more general than the results of Okhawa and Uemura,[21] who derived a zero-field splitting proportional to $\langle dV/dz \rangle$ and obviously neglected the influence of the interface electric fields $\sim \delta g^* \langle \Theta(-z)/dz \rangle$. Ando's argument[22] that the average electric field in the conduction band vanishes ($\langle dU_c/dz \rangle = 0$) and that the spin splitting should be very small is not correct since only the derivatives of $U_v(z), U_\Delta(z), \ldots$ appear in $\langle dg/dz \rangle$.

In Fig. 4 the splitting for $k_\perp = k_F = \sqrt{\pi N}$ is plotted as a function of the electron density for two δ_c values and $N_d = 10^{10}/\text{cm}^2$ (solid line) and $N_d = 3 \times 10^{10}/\text{cm}^2$ (dashed line). Although the depletion charge dependence is again relatively strong, the influence of the barrier height is considerably stronger than it was for the effective mass. A higher valence-band discontinuity results in a stronger splitting. Therefore a detailed experimental study of the spin splitting at zero field can be used to determine the interface parameters.

Stein and Klitzing[17] performed electron-spin-resonance experiments in GaAs-GaAlAs heterostructures at $H > 2.5$ T and found a significant deviation from the three-dimensional values. Their extrapolation to zero magnetic field yields a splitting of the order of our theoretical values. However, the extrapolation to $H = 0$ is not unique, so that this comparison cannot be considered as reliable. Figure 5 shows a direct comparison of the data of Stein and Klitzing (the magnetic field perpendicular to the surface) with our theory. The spin splitting is plotted as a function of the magnetic field for $N_{el} = 4.6 \times 10^{11}/\text{cm}^2$, $N_d = 6 \times 10^{10}/\text{cm}^2$, $\delta_c/\delta E_g = 0.6$ (solid line), and $\delta_c/\delta E_g = 0.85$ (dotted line). The dashed line indicates the bulk GaAs value. The "diagonal" spin splitting at high magnetic fields depends only weakly on the barrier height, and a stronger penetration into the barrier reduces the splitting, since δg^* is positive.

Although about 60% of the deviation from the bulk GaAs value are well described, there remains an unexplained discrepancy between our model and the experimental results. An improvement is expected from more exact wave functions including exchange and correlation effects in the energy calculation, warping effects,[23] and from a more detailed investigation of the Bloch function matching at the interface.

Stein and Klitzing also observed an increase of the resonance energy when the carrier concentration was increased by light illumination. The present theory can unambiguously explain the origin of the additional charge in the channel. In principle, this charge can be due to a transfer either of depletion charges or of charges from the GaAlAs across the barrier. In the first case the potential $V(z)$ becomes considerably weaker; in the second case it becomes stronger. Only a weaker potential will result in

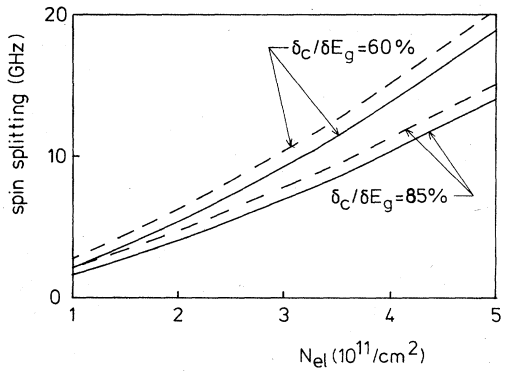

FIG. 4. Spin splitting at zero magnetic field versus charge density for electrons at the Fermi surface with wave vector k_F, for two barrier heights and for $N_d = 10^{10}/\text{cm}^2$ (solid lines) and $N_d = 3 \times 10^{10}/\text{cm}^2$ (dashed lines).

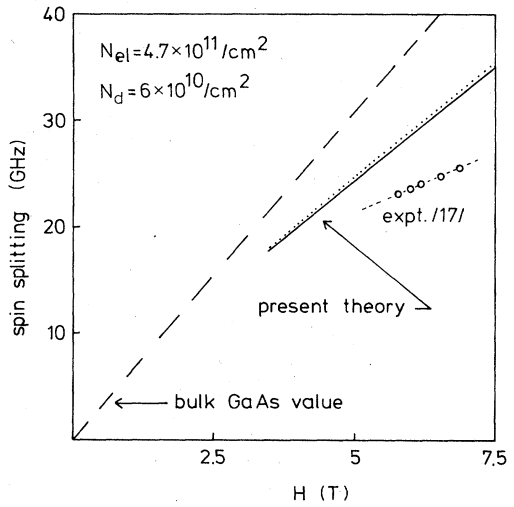

FIG. 5. Spin splitting versus magnetic field for electrons in the first Landau level, for $\delta_c/\delta E_g = 60\%$ (solid line) and $\delta_c/\delta E_g = 85\%$ (dotted line). The present theory explains about 60% of the experimental deviation from the bulk GaAs value.

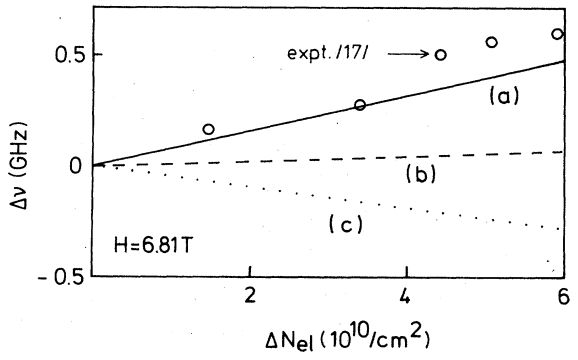

FIG. 6. Variation of the spin-resonance frequency when additional charges ΔN_{el} are introduced in the channel by light illumination. The experiment (Ref. 17) can only be explained if the new charges are taken from the depletion layer [curve (a)]. Cases (b) and (c) show for comparison the result if 50% and 100% of the charges come from the GaAlAs. Before illumination, the electron density was $N_{el} = 4.66 \times 10^{11}/\text{cm}^2$ and the depletion density was $N_d = 6 \times 10^{10}/\text{cm}^2$. The barrier height is $\delta_c = 0.6 \times \delta E_g$, and a higher value yields the same result.

an increased spin splitting, since in the GaAs-GaAlAs heterostructure the nonparabolicity reduces the effective g factor. In Fig. 6 three cases are compared with the experimental results. The magnetic field is 6.81 T and $\delta_c/\delta E_g = 60\%$. The electron and depletion charge values at the beginning of the experiment are $N_{\rm el} = 4.66 \times 10^{11}/{\rm cm}^2$ and $N_d = 6 \times 10^{10}/{\rm cm}^2$. Curve (a) describes the situation when all charges are taken from the depletion layer. In case (b) 50% and in case (c) 100% of the charges are taken from the GaAlAs material. It is seen that only a reduction of the depletion charges can explain the experimental data.

As a conclusion, I can state that a careful analysis of cyclotron-resonance and spin-flip experiments reveals new information on the band structure in two-dimensional systems. From a detailed study of the energy fine structure, band-edge discontinuities as well as the mechanisms of charge transfer at light illumination can be determined.

ACKNOWLEDGMENTS

I would like to thank Professor E. Gornik and Professor W. Zawadzki for extensive and useful discussions.

APPENDIX A

For the band-edge Bloch features $u_{l,0}$ the following states are chosen, which include the spin-orbit interaction to first order of perturbation theory:

$$u_1 = iS\mathcal{S}(\uparrow), \quad \epsilon_{10} = 0 \tag{A1}$$

$$u_2 = iS\mathcal{S}(\downarrow), \quad \epsilon_{20} = 0 \tag{A2}$$

$$u_3 = R_+\mathcal{S}(\uparrow), \quad \epsilon_{30} = -E_0 \tag{A3}$$

$$u_4 = R_-\mathcal{S}(\downarrow), \quad \epsilon_{40} = -E_0 \tag{A4}$$

$$u_5 = \frac{1}{\sqrt{3}} R_-\mathcal{S}(\uparrow) + (\tfrac{2}{3})^{1/2} Z\mathcal{S}(\downarrow), \quad \epsilon_{50} = -E_0 \tag{A5}$$

$$u_6 = -\frac{1}{\sqrt{3}} R_+\mathcal{S}(\downarrow) + (\tfrac{2}{3})^{1/2} Z\mathcal{S}(\uparrow), \quad \epsilon_{60} = -E_0 \tag{A6}$$

$$u_7 = -(\tfrac{2}{3})^{1/2} R_-\mathcal{S}(\uparrow) + \frac{1}{\sqrt{3}} Z\mathcal{S}(\downarrow), \quad \epsilon_{70} = -E_0 - \Delta_0 \tag{A7}$$

$$u_8 = (\tfrac{2}{3})^{1/2} R_+\mathcal{S}(\downarrow) + \frac{1}{\sqrt{3}} Z\mathcal{S}(\uparrow), \quad \epsilon_{80} = -E_0 - \Delta_0 \tag{A8}$$

where $R_\pm = (X \pm iY)/\sqrt{2}$ and the symbols $\mathcal{S}(\uparrow)$ and $\mathcal{S}(\downarrow)$ mean spin-up and spin-down functions, respectively. The angular momentum is quantized in the z direction and the zero of energy is chosen at the bottom of the conduction band. S and (X,Y,Z) are periodic functions which transform like atomic s and p functions under the tetrahedral group at the Γ point.

For the magnetic field in z direction, generalized momentum operators are defined:

$$\hat{P} = \mathbf{p} + \frac{e}{c}\mathbf{A}\,, \tag{A9}$$

which obey the following commutation relations:

$$[\hat{P}_x, \hat{P}_y] = -i\frac{\hbar^2}{l^2}, \quad [P_z, P_x] = [P_z, P_y] = 0\,. \tag{A10}$$

In Landau gauge vector potential is $\mathbf{A} = (-H_y, 0, 0)$ and $l = \sqrt{\hbar c/eH}$ is the Landau radius.

APPENDIX B

The different expectation values that must be evaluated are split into the two contributions from the integral smaller and larger than zero:

$$\langle A \rangle = \langle A \rangle_- + \langle A \rangle_+\,. \tag{B1}$$

One obtains

$$\langle \alpha \rangle = \alpha_-\rho_- + \alpha_+\rho_+\,, \tag{B2}$$

$$\rho_- = C, \quad \rho_+ = 1 - \rho_-\,, \tag{B3}$$

$$\left\langle \frac{1}{1+\delta m\Theta(-z)} \right\rangle = \frac{\rho_-}{1+\delta m} + \rho_+\,, \tag{B4}$$

$$\langle V \rangle = \langle V \rangle_- + \langle V \rangle_+\,, \tag{B5}$$

$$\langle V \rangle_- = \frac{4\pi e^2}{\kappa_s} \left[\frac{-C}{c} \right] \left[N_d + N_{\rm el} \left[1 + \frac{C}{2} \right] \right], \tag{B6}$$

$$\langle V \rangle_+ = \frac{4\pi e^2}{\kappa_s} \left\{ \frac{B}{b} N_d(6 + 4k + k^2) + N_{\rm el} \left[\left[\frac{-C}{c} \right] \rho_+ + \frac{B^2}{b} (\tfrac{33}{4} + \tfrac{25}{2}k + \tfrac{17}{2}k^2 + 3k^3 + \tfrac{1}{2}k^4) \right] \right\}, \tag{B7}$$

$$\langle V\alpha \rangle = \alpha_- \langle V \rangle_- + \alpha_+ \langle V \rangle_+\,, \tag{B8}$$

$$-\left\langle \frac{d}{dz} \left[\frac{1}{1+\delta m\Theta(-z)} \right] \frac{d}{dz} \right\rangle = \frac{\tau_-}{1+\delta m} + \tau_+\,, \tag{B9}$$

$$\tau_- = \frac{c^2}{4} C\,, \tag{B10}$$

$$\tau_+ = \frac{b^2}{4} B(2-2k+k^2) , \tag{B11}$$

$$\left\langle \frac{d}{dz} V\alpha \frac{d}{dz} \right\rangle = \alpha_- \left\langle \frac{d}{dz} V \frac{d}{dz} \right\rangle_- + \alpha_+ \left\langle \frac{d}{dz} V \frac{d}{dz} \right\rangle_+ , \tag{B12}$$

$$-\left\langle \frac{d}{dz} V \frac{d}{dz} \right\rangle_- = \frac{4\pi e^2}{\kappa_s} \left[-\frac{c}{4} C \right] \left[N_d + N_{\rm el} \left[1 + \frac{C}{2} \right] \right] , \tag{B13}$$

$$-\left\langle \frac{d}{dz} V \frac{d}{dz} \right\rangle_+ = \frac{4\pi e^2}{\kappa_s} \left[\frac{b}{4} B \right] \left[N_d(2+k^2) + N_{\rm el} B\left(\tfrac{11}{4} + \tfrac{3}{2}k + \tfrac{11}{2}k^2 + k^3 + \tfrac{1}{2}k^4\right) - N_{\rm el} \frac{b}{c} C(2-2k+k^2) \right] , \tag{B14}$$

$$\langle \mathscr{H}_s \rangle = \tfrac{1}{2}\mu_B [g_0^* + \delta g^* \rho_- + \beta_- \langle V \rangle_- + \beta_+ \langle V \rangle_+] . \tag{B15}$$

[1] J. M. Luttinger and W. Kohn, Phys. Rev. **97**, 869 (1955).
[2] E. O. Kane, J. Phys. Chem. Solids **1**, 249 (1957).
[3] C. Hermann and C. Weisbuch, Phys. Rev. B **15**, 823 (1977).
[4] B. Vinter, Phys. Rev. Lett. **35**, 1044 (1975).
[5] L. J. Sham and M. Nakayama, Phys. Rev. **20**, 734 (1979).
[6] Y. Takada, K. Arai, N. Uchimura, and Y. Uemura, J. Phys. Soc. Jpn. **49**, 1851 (1980).
[7] G. E. Marques and L. J. Sham, Surf. Sci. **113**, 131 (1982).
[8] W. Zawadzki, J. Phys. C **16**, 229 (1983).
[9] R. Dingle, in *Festkörperprobleme (Advances in Solid State Physics)*, edited by H. J. Queisser (Pergamon/Vieweg, Braunschweig, 1975), Vol. 15, p. 21.
[10] R. C. Miller, D. A. Kleinman, and A. C. Gossard, Phys. Rev. B **29**, 7085 (1984).
[11] T. Ando, J. Phys. Soc. Jpn. **51**, 3893 (1982).
[12] T. Ando, J. Phys. Soc. Jpn. **51**, 3900 (1982).
[13] G. Bastard, Surf. Sci. **142**, 284 (1984).
[14] F. Stern and S. Das Sarma, Phys. Rev. B **30**, 840 (1984).
[15] Richard A. Morrow and Kenneth R. Brownstein, Phys. Rev. B **30**, 678 (1984).
[16] W. Seidenbusch, G. Lindemann, R. Lassnig, J. Edlinger, and E. Gornik, Surf. Sci. **142**, 375 (1984).
[17] D. Stein and K. V. Klitzing, Phys. Rev. Lett. **51**, 130 (1983).
[18] W. Zawadzki, in *Narrow Gap Semiconductors, Nimes, 1979,* edited by W. Zawadzki (Springer, New York, 1980), p. 85.
[19] D. J. Ben Daniel and C. B. Duke, Phys. Rev. **152**, 683 (1966).
[20] *Landolt-Börnstein, New Series,* edited by O. Madelung (Springer, New York, 1982), Vol. III/17a, pp. 218 and 334.
[21] F. J. Okhawa and Y. Uemura, in Proceedings of the Second International Conference on Solid Surfaces, 1974 [Jpn. J. Appl. Phys. Suppl. **22**, 355 (1974)].
[22] T. Ando, A. B. Fowler, and F. Stern, Rev. Mod. Phys. **54**, 599 (1982).
[23] U. Rössler, Solid State Commun. **49**, 943 (1984).